Available online at www.sciencedirect.com
ScienceDirect
Journal of Molecular Catalysis A: Chemical 281 (2008) 14–23
JOURNAL OF MOLECULAR CATALYSIS A: CHEMICAL
www.elsevier.com/locate/molcata

Probing reaction pathways on model catalyst surfaces: Vinyl acetate synthesis and olefin metathesis

Feng Gao, Yilin Wang, Florencia Calaza, Dario Stacchiola, Wilfred T. Tysoe *

Department of Chemistry and Biochemistry, and Laboratory for Surface Studies, University of Wisconsin-Milwaukee, Milwaukee, WI 53211, USA

Available online 1 September 2007

Abstract

The reaction pathway for the palladium-catalyzed synthesis of vinyl acetate from acetic acid, ethylene and oxygen is investigated using reflection–absorption infrared spectroscopy by monitoring the rate of acetate titration by gas-phase ethylene. This reveals that acetate species are removed by reaction with gas-phase ethylene resulting in vinyl acetate formation. Reaction with C_2D_4 reveals a large (∼6) isotope effect indicating that hydrogen is involved in the rate-limiting step. This also results in the appearance of an infrared feature that is assigned to an acetoxyethyl-palladium intermediate. Acetate reaction rates are different for the isotopomers, CH_2CD_2 and CHDCHD. These observations are consistent with a reaction pathway first proposed by Samanos in which ethylene reacts with an acetate species to form an acetoxyethyl-palladium intermediate, which then reacts to form vinyl acetate by a β-hydride elimination reaction. The Hérisson–Chauvin pathway for olefin metathesis, which proposes that reaction occurs between a surface carbene and alkene to form a C_3 metallacycle, which decompose by the reverse of this pathway to form metathesis products, is tested on a MoAl alloy formed by reactions with $Mo(CO)_6$ with an alumina thin film grown on a refractory metal substrate. This is the accepted pathway in homogeneous phase, and is demonstrated to occur on the alloy surface by grafting intermediates using iodine-containing precursors.
© 2007 Elsevier B.V. All rights reserved.

Keywords: Pd(1 1 1); Infrared spectroscopy; Vinyl acetate synthesis; Alloy; Olefin metathesis; Reaction pathway

1. Introduction

The ability to understand catalytic reaction pathways in detail requires kinetic measurements to be made on the elementary reaction steps on model systems that mimic the realistic catalyst. When the heats of adsorption of the reactants are larger than, or of the same magnitude as the activation energy of the surface reaction step, ultrahigh vacuum techniques such as temperature-programmed desorption can be used to probe elementary step reaction kinetics. If this is not the case, the reactants merely desorb without reacting. In such cases, elementary reaction steps can only be explored when the surface is pressurized by the reactant and requires the nature of the surface to be probed in the presence of high pressures of one or more of the reactants, therefore requiring surface-sensitive techniques that can operate under high-pressure conditions. Photon-based methods such as infrared spectroscopy are ideally suited to such experiments and its utility is illustrated in the following using the example of the palladium-catalyzed synthesis of vinyl acetate monomer (VAM) from acetic acid, ethylene and oxygen [1]:

$$CH_3COOH + C_2H_4 + (1/2)O_2 \rightarrow CH_3COOC_2H_3 + H_2O \quad (1)$$

Since this reaction is catalyzed by supported palladium, and a Pd(1 1 1) single crystal has been shown to catalyze the reaction [2], the mechanism of vinyl acetate synthesis is studied on a Pd(1 1 1) single crystal. In many cases, however, single crystal substrates are not faithful models of the working catalyst and model systems that more closely mimic the supported system must be synthesized. An example of this strategy is illustrated for model catalysts systems grown on an oxide support, in this case, by the reaction of molybdenum hexacarbonyl with alumina films grown on a refractory metal support [3–11]. This results in the formation of a number of phases, depending on temperature and the nature of the support. However, of particular interest is a molybdenum–aluminum alloy system, which has been demonstrated to be extremely active for the migratory insertion of methylene into surface alkyl groups, resulting in the detection of alkenes up to C_4 after grafting methylene species

* Corresponding author. Tel.: +1 414 229 5222; fax: +1 414 229 5036.
E-mail address: wtt@uwm.edu (W.T. Tysoe).

1381-1169/$ – see front matter © 2007 Elsevier B.V. All rights reserved.
doi:10.1016/j.molcata.2007.08.026

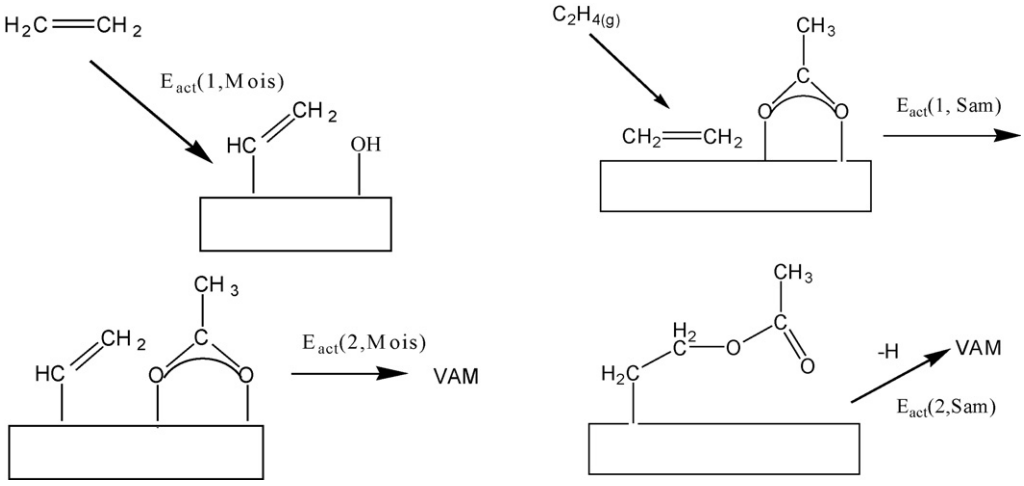

Scheme 1. Illustrations of the proposed Moiseev and Samanos reaction pathways.

onto the surface [12]. It has been suggested that, in homogeneous phase, olefin metathesis reactions proceed via a similar migratory insertion of a carbene into the C–metal bond of an alkene to form a metallacycle [13–30]. The reverse of this reaction, metallacycle decomposition to evolve an alkene leaving a surface carbene, results in the formation of metathesis products. The efficacy of the model alloy for migratory insertion reactions allows the carbene–metallacycle pathway to be explored in ultrahigh vacuum.

2. Experimental

All experiments were carried out under ultrahigh vacuum conditions to allow clean, well-characterized samples to be obtained. A wide range of surface analysis techniques have been used to follow the reaction pathways and these, along with the sample preparation and cleaning techniques have been described in detail elsewhere [31]. All gases used for the experiments were of 99+% purity and were transferred to glass bottles, which were attached to the gas-handling line for introduction into the vacuum chamber and their purities were determined mass spectroscopically. The purities of the key compounds used in this work were as follows: C_2H_4 (Matheson, Research Grade), acetic acid (Aldrich, 99.99+%), C_2D_4 (CIL, 98% D), CD_2CH_2 (CDN, 99% D), CHDCHD (CDN, *cis/trans* mixture, 99% D) and $^{18}O_2$ (CIL, 95% $^{18}O_2$), molybdenum hexacarbonyl (Aldrich, 99%), propylene (Matheson, 99.5%), d_6-propylene, CD_2=CH–CH_3, CH_2=CH–CD_3 (Cambridge Isotope, ≥99% D), 1-iodopropane and 1,3-diiodopropane (Aldrich, 99%).

3. Results and discussion

3.1. The reaction pathway for the synthesis of vinyl acetate on Pd(1 1 1)

Two alternative mechanisms have been proposed to describe the palladium-catalyzed formation of VAM. The first, suggested by Samanos, involves the coupling of ethylene directly with chemisorbed acetate on Pd [32]. The resulting acetoxyethyl-palladium intermediate then undergoes a β-hydride elimination reaction to form vinyl acetate. Alternatively, ethylene could first dehydrogenate to form a vinyl-palladium intermediate, which then would couple with a surface acetate species to form VAM directly. This is known as the Moiseev mechanism [33] and these pathways are illustrated in Scheme 1.

The structures of adsorbed η^2-acetate [34] and ethylene [35] have been determined separately on Pd(1 1 1) using low-energy electron diffraction (LEED) and reflection absorption infrared spectroscopy (RAIRS) [34–37]. These experiments reveal that the acetate adsorbs with the molecular plane oriented perpendicular to the palladium surface with the oxygen atoms located almost above palladium sites such that the carbon atom in the carboxylate is positioned directly above a bridge site. The saturation coverage is ∼1/3 of a monolayer (where coverages are referenced to the palladium atom site density on the surface) [38]. Ethylene is substantially rehybridized on clean Pd(1 1 1) and also adsorbs at the bridge site on the clean surface so that the adsorption of di-σ-bonded ethylene should therefore be blocked by the acetate species [35].

The work outlined in the following addresses the question of the nature of the reaction pathway primarily using isotopically labeled reactants. A Pd(1 1 1) surface saturated with acetate species was pressurized with ethylene (P(ethylene) = 2×10^{-7} Torr) and the integrated intensity of the acetate feature at 1414 cm^{-1} followed as a function of time at a sample temperature of 327 K, where the data for reaction with C_2H_4 (■) are displayed in Fig. 1. Separate calibration experiments show that the integrated intensity of this feature is, to a good approximation, proportional to coverage. This clearly shows that surface acetate species react with gas-phase ethylene and temperature-programmed desorption experiments performed in the presence of gas-phase ethylene confirm that these react to form vinyl acetate [39]. In order to investigate whether the rate-limiting step involves hydrogen, the acetate species on Pd(1 1 1) was also reacted with C_2D_4 (●) CD_2CH_2 (▲) and CHDCHD (▼) and the resulting plots of acetate coverage *versus* time are also displayed in Fig. 1. Shown as lines on this figure are fits to a kinetic model that will be discussed in greater

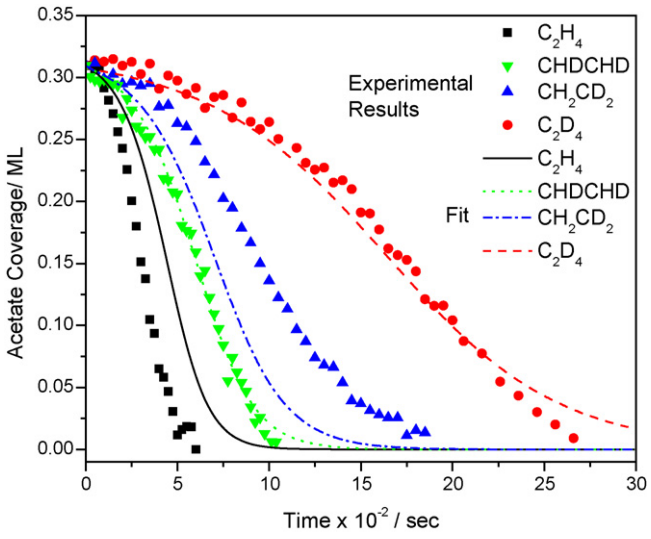

Fig. 1. Plot of the time dependence of the coverage of the acetate species measured from the intensity of the 1414 cm^{-1} acetate mode for the reaction of C_2H_4 (■), CH_2CD_2 (▲), CHDCHD (▼) and C_2D_4 (●) with acetate species on Pd(1 1 1) with an ethylene pressure of 2×10^{-7} Torr at a reaction temperature of 327 K.

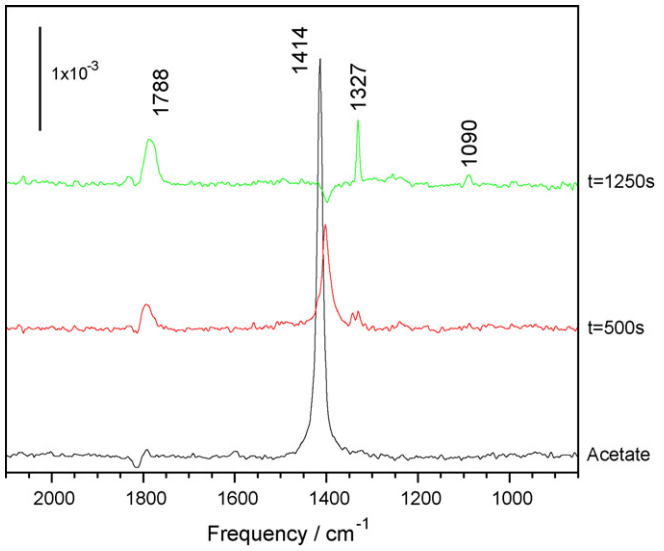

Fig. 2. Infrared spectra of acetate species on Pd(1 1 1) reacted with ethylene at a pressure of $\sim 2 \times 10^{-7}$ Torr at 327 K for various times collected for 1000 scans to improve the signal-to-noise ratio. The reaction times are indicated adjacent to the corresponding spectrum.

detail below. Clearly there are substantial differences in the reaction rates between C_2H_4 and C_2D_4 indicating that hydrogen is involved in the rate-limiting step. Interestingly, the reaction rates for d_2-ethylene isotopomers depend on the deuterium position: reaction is slower for the 1,1-dideuterated reactant than for 1,2-dideuteroethylene. The implication of this result will be discussed in greater detail below.

Experimental data shown in Fig. 1 were collected for 100 scans to allow a large number of data points to be collected for the kinetic measurements. Similar experiments were carried out as a function of time, but now by collecting spectra for 1000 scans to yield better signal to noise. The resulting spectra are displayed in Fig. 2 for reaction at 327 K on clean Pd(1 1 1) and show a decrease in the intensity of the 1414 cm^{-1} feature due to the removal of acetate species noted in Fig. 1, along with the formation of ethylidyne (from the peak at 1327 cm^{-1}) [39]. An additional feature is observed to grow at $\sim$1778 cm^{-1}, in the C=O stretching region. Heating an acetate-covered surface to this temperature in the absence of ethylene does not result in the appearance of this peak. Shown in Fig. 3 are a series of infrared spectra collected at identical temperatures and ethylene pressures until the acetate species had been removed using: (b) C_2H_4 (reproducing the spectrum in Fig. 2), (c) C_2H_4 on an ^{18}O-covered surface formed by exposing clean Pd(1 1 1) to $^{18}O_2$ and (d) using C_2D_4. Shown for comparison is the spectrum of CO on Pd(1 1 1) (Fig. 3a), where the CO exposure was selected to yield a similar intensity to the features produced by reaction between ethylene and adsorbed acetate species. This confirms that these features are not due to CO adsorbed from the background. The peaks at 1330 and 1090 cm^{-1} in these spectra (Fig. 3(b) and (c)) are due to ethylidyne species [39]. These data also show that surface oxygen does not appear to be involved in the surface reaction, but the 1778 cm^{-1} feature shifts to $\sim$1718 cm^{-1} when the reaction is carried out using C_2D_4.

In order to establish whether the 1718 cm^{-1} feature is due to an isotope shift of the 1778 cm^{-1} mode, and to aid in establishing the nature of the species giving rise to the $\sim$1778 cm^{-1} feature, both d_6- and normal vinyl acetate were adsorbed on ethylidyne-covered Pd(1 1 1) at 300 K for ethylidyne coverages of 0.25 (saturation) and $\sim$0.1 monolayers. The resulting spectra are shown in Fig. 4 for normal (Fig. 4(a)) and perdeuterated (Fig. 4(b)) VAM. The spectra reveal that VAM exhibits a single feature at $\sim$1778 cm^{-1} for both normal and perdeuterated vinyl acetate on an ethylidyne-saturated Pd(1 1 1) surface. This observation provides confirmation that the reaction between ethylene and adsorbed acetate species yields vinyl acetate,

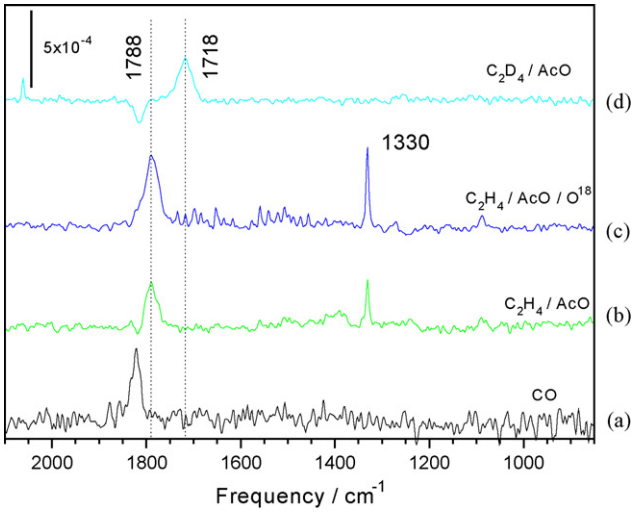

Fig. 3. Infrared spectra of acetate species reacted with ethylene at 327 K until the acetate had been removed, for reaction with (b) C_2H_4 with acetate-covered Pd(1 1 1), (c) C_2H_4 with acetate-covered ^{18}O-(2 × 2)/Pd(1 1 1) (d) C_2D_4 with acetate-covered Pd(1 1 1). Shown for comparison is the infrared spectrum of CO on Pd(1 1 1) (a).

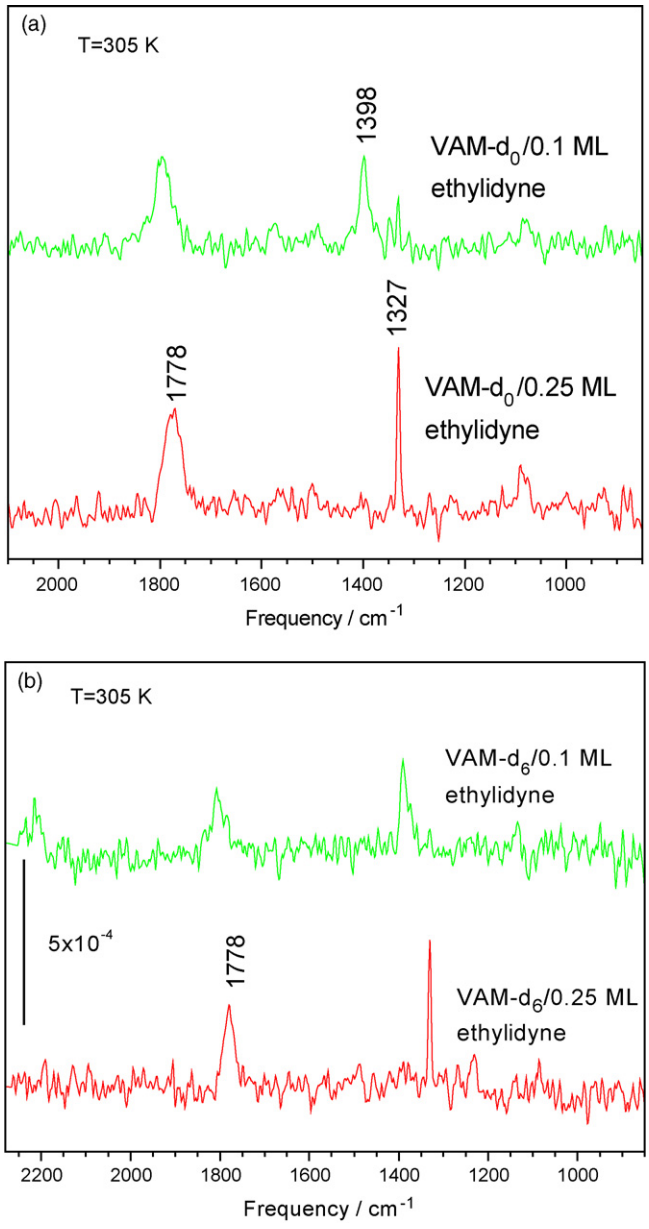

Fig. 4. Infrared spectrum of (a) d_0-vinyl acetate adsorbed on 0.25 and 0.1 mL of ethylidyne and (b) d_6-vinyl acetate on 0.25 and 0.1 mL of ethylidyne at 305 K.

in accord with previous temperature-programmed desorption results where gas-phase vinyl acetate was detected [39]. It should be emphasized that this spectrum is considerably different from that of vinyl acetate on clean Pd(1 1 1) [40], which exhibits a large number of features, one of which is a C=O stretching mode at ~1760 cm^{-1}. Furthermore, heating this surface to ~300 K results in substantial vinyl acetate decomposition. Evidently, the presence of ethylidyne on the surface inhibits vinyl acetate decomposition. Indeed, lowering the ethylidyne coverage to ~0.1 ML (Fig. 4) results in some decomposition as evidenced by the feature appearing at ~1398 cm^{-1}. However, the feature at ~1718 cm^{-1} is clearly not due to vinyl acetate adsorbed on the surface. The presence of this feature does, however, provide a clue to the reaction pathway. In the Moiseev pathway, the only species expected to be present on the surface are ethylene, vinyl and acetate species, and vinyl acetate, and the ~1718 cm^{-1} mode is due to none of these. The species participating in the Samanos pathway are ethylene, acetate, vinyl acetate and the acetoxyethyl-palladium intermediate resulting from insertion of ethylene into the acetate–Pd bond (see Scheme 1). Such an acetoxyethyl-palladium intermediate will have a C=O stretching frequency lower than that of vinyl acetate [41,42] implying that the 1718 cm^{-1} mode could be due to the presence of the reaction intermediate. The appearance of this feature can be rationalized on the basis of the Samanos pathway [32]. Since the acetoxyethyl-palladium intermediate decomposes to form vinyl acetate *via* a β-hydride elimination reaction, the rate of this reaction will be slowed substantially by deuteration at the β position accounting for its appearance when C_2D_4 reacts with surface acetate species. Indeed, further reaction with C_2D_4 results in a loss in intensity of the 1718 cm^{-1} mode and the growth of a mode at ~1788 cm^{-1} in accord with this proposal.

These results demonstrate that ethylene reacts with acetate species on Pd(1 1 1) to yield vinyl acetate [39], consistent with the detection of vinyl acetate adsorbed on ethylidyne-covered Pd(1 1 1) (Fig. 4) by infrared spectroscopy following reaction between ethylene and acetate species. The feature appearing at ~1718 cm^{-1} after reaction between C_2D_4 and acetate species is assigned to the presence of an acetoxyethyl-palladium intermediate arising from a reaction between gas-phase ethylene and adsorbed acetate. This assignment is based on the observation that the C=O stretching frequency of alkyl acetate is ~60 cm^{-1} lower in frequency than for vinyl acetate [41,42]. These data strongly suggest that vinyl acetate is formed by the insertion of ethylene into the O–Pd bond of the acetate species followed by β-hydride elimination to yield vinyl acetate; the Samanos pathway [32].

Additional evidence for the Samanos pathway comes from the isotope data of Fig. 1. Clearly, as noted above, hydrogen is involved in the rate-limiting step since the acetate removal rate when using C_2D_4 is substantially lower than when using C_2H_4. Of greater interest, however, are the different acetate removal rates for d_2-ethylene, where CD_2CH_2 reacts more slowly than does CHDCHD. This observation allows

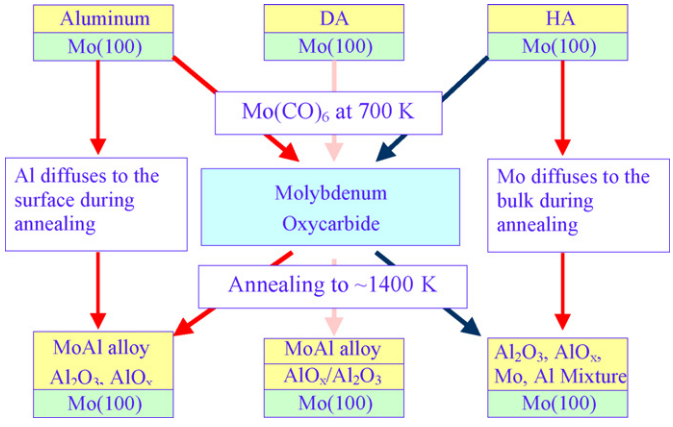

Fig. 5. Schematic diagram summarizing the films formed on various alumina surfaces by reaction with molybdenum hexacarbonyl.

us to immediately exclude the Moiseev model since, in this case, the rate-limiting step, which involves hydrogen, must be hydrogen abstraction from the ethylene to form the vinyl species. A fit to the experimental data (Fig. 1) yields value of $k_i(H)/k_i(D) \sim 6$. This is a reasonable value for a primary isotope effect. In the case of reaction with d_2-ethylene, the rate constant should be $(k_i(H) + k_i(D))/2$ yielding an isotope effect of $2/(1 + (k_i(D))/k_i(H)) \sim 1.7$. This will be the same irrespective of the location of deuterium, in contrast to what is observed experimentally.

At first sight, a similar effect should occur with the Samanos model. In the case of reaction with CD_2CH_2, there is an equal probability of CH_2 or CD_2 being in the β-position in the acetoxyethyl-palladium intermediate yielding an isotope effect of ∼1.7, while for CHDCHD there will always be a CHD group at the β-position, similarly yielding an isotope effect of ∼1.7.

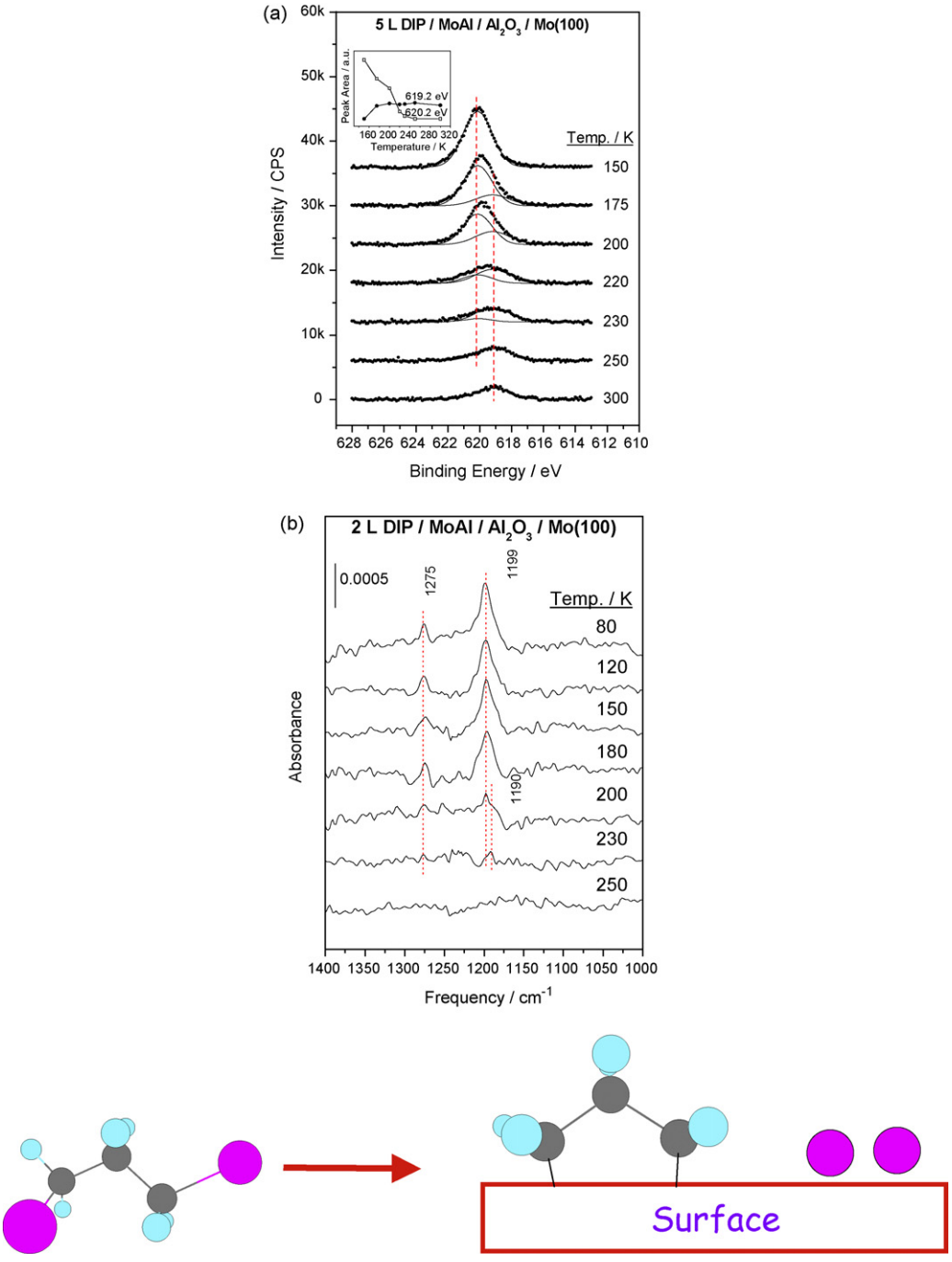

Fig. 6. (a) $I3d_{5/2}$ photoelectron spectra of 5 L of 1,3-diiodopropane adsorbed on a MoAl surface at 150 K and heated to various temperatures, where the annealing temperatures are displayed adjacent to the corresponding spectrum. Shown as an inset are the areas of the $I3d_{5/2}$ signals from 1,3-diiodopropane (centered at 620.2 eV) and atomic iodine (centered at 619.2 eV) plotted as a function of temperature. (b) Reflection–absorption infrared spectra (RAIRS) following the adsorption of 2 L of 1,3-diiodopropane on a MoAl alloy as a function of annealing temperature, where the annealing temperatures are displayed adjacent to the corresponding spectrum. The surface chemistry is indicated schematically at the bottom of the figure.

However, if the acetoxyethyl-palladium intermediate blocks the adsorption of ethylene, any acetoxyethyl-palladium intermediates formed from CH_2CD_2 with two deuteriums in the β-position will decompose more slowly than those with hydrogens at that position, and block ethylene adsorption to a larger extent. For reaction with CHDCHD, there will always be hydrogen at the β-position, so that the intermediate can decompose more rapidly resulting in less blocking of the ethylene adsorption by the intermediate. This suggests that reaction with CD_2CH_2 should be slower than that with CHDCHD as found experimentally (Fig. 1). The data in Fig. 1 were fit using a simple kinetic model that assumes that ethylene adsorption is blocked by both surface acetate species and the acetoxyethyl-palladium intermediate and that the reaction rate is given by $k \times \theta(\text{ethylene}) \times \theta(\text{acetate})$, where θ refers to the surface coverage, and k is the reaction rate constant. Reactions were carried out at a sufficiently high pres-

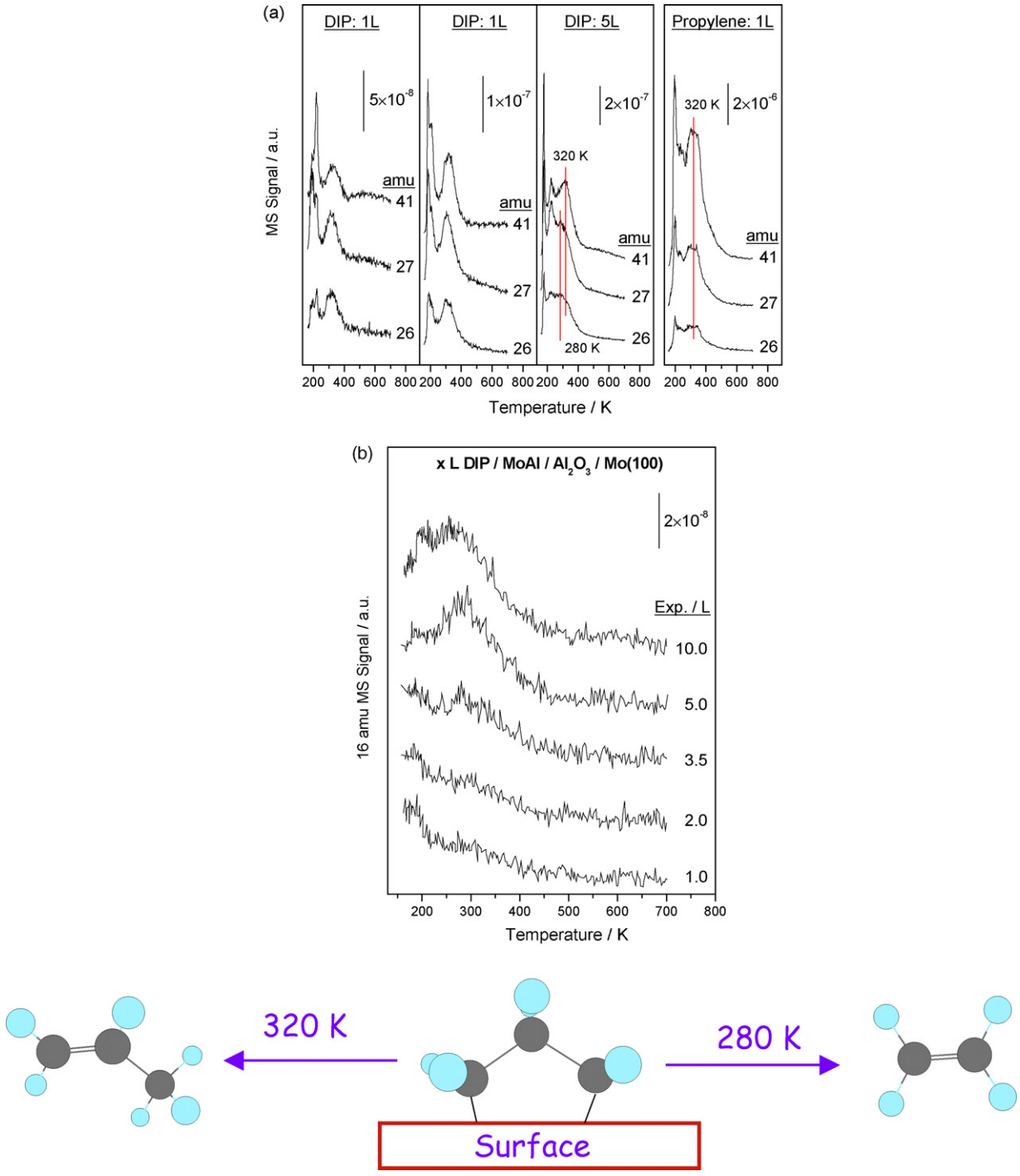

Fig. 7. Temperature-programmed desorption spectra of various exposures of 1,3-diiodopropane adsorbed on a MoAl alloy surface, monitoring (a) 41 (propylene), and 26 and 27 amu (ethylene) and (b) 16 (methane). The 1,3-diiodopropane exposures are marked adjacent to the corresponding spectrum. The surface chemistry is indicated schematically at the bottom of the figure.

sure to saturate the surface with ethylene. Since acetate species block ethylene adsorption, the ethylene coverage was taken to be $1-\theta$(acetate). The rate constant is varied depending on the number of deuteriums in the β position of the acetoxyethylpalladium intermediate resulting in a change in its coverage and a concomitant change in reaction rate. The results of this simple kinetic model yield the lines plotted in Fig. 1. While the fits are not perfect, they effectively reproduce the different rates found for CH_2CD_2 and CHDCHD.

3.2. The reaction pathway for the olefin metathesis on molybdenum–aluminum alloys

Models of alumina-supported catalysts can be synthesized by reacting $Mo(CO)_6$ with alumina films grown on a Mo(1 0 0) substrate [3–11]. The alumina film is grown by evaporating aluminum onto the metal support and oxidizing using water to yield hydroxylated alumina. This can be dehydroxylated by heating to various temperatures in ultrahigh vacuum to desorb water. The $Mo(CO)_6$ decarbonylation pathway has been extensively investigated. However, reacting the carbonyl with the alumina surface at ~700 K results in a number of surface phases summarized in Fig. 5. Of particular interest is the molybdenum oxycarbide phase that reduces the alumina substrate on heating to ~1400 K to desorb predominantly CO and results in the formation of a molybdenum–aluminum alloy. It has been demonstrated previously that this surface is exceptionally active for the migratory insertion of methylene species into adsorbed alkyls to form higher hydrocarbons [12]. This property is used to examine the migratory insertion of methylene species into ethylene adsorbed on the alloy to form C_3 surface metallacycles. In the homogeneous-phase metathesis pathway, this is proposed to decompose by the reverse of the formation pathway to evolve an alkene and leave the carbene on the surface [13–30]. In order to explore this chemistry on the MoAl alloy, C_3 metallacycles were grafted onto the surface by exposure to 1,3-diidodopropane. This is now a well-established strategy for grafting reaction intermediates onto surfaces, since the C–I bond is relatively weak compared to the C–H bonds and is preferentially cleaved to deposit the organic fragment along with chemisorbed iodine. The strategy is illustrated graphically by the schematic diagram at the bottom of Fig. 6. Shown in Fig. 6(a) are a series of iodine X-ray photoelectron spectra collected following the adsorption of 1,3-diidodopropane on the alloy and annealing to higher temperature [43]. Following adsorption at ~150 K, the binding energy indicates that the iodine is bonded to carbon. However, heating the sample reduces the intensity of this feature leading to an additional iodine feature appearing at lower binding energy due to iodine adsorbed on the alloy surface. The iodine spectra of 1,3-diidodopropane and adsorbed iodine are fit to Lorentzian profiles and the spectra at intermediate temperatures are fit to a linear combination of these features. The reflection–absorption infrared spectrum collected following the adsorption of 1,3-diidodopropane and heating to various temperatures (Fig. 6(b)) is also consistent with the presence of a C_3 metallacycle on the surface since features are in accord with the continued presence of a C_3H_3 moiety.

The reaction pathways are probed using temperature-programmed desorption (TPD), where the TPD profiles are displayed for the 41, 27 and 26 amu signals in Fig. 7(a) following 1,3-diidodopropane adsorption at ~100 K. The signal at 41 amu is due to propylene desorption suggesting that a portion of the metallacycle decomposes by a hydrogen-transfer reaction to form propylene. Shown for comparison is the TPD profile for propylene itself adsorbed on the alloy, which has the most intense

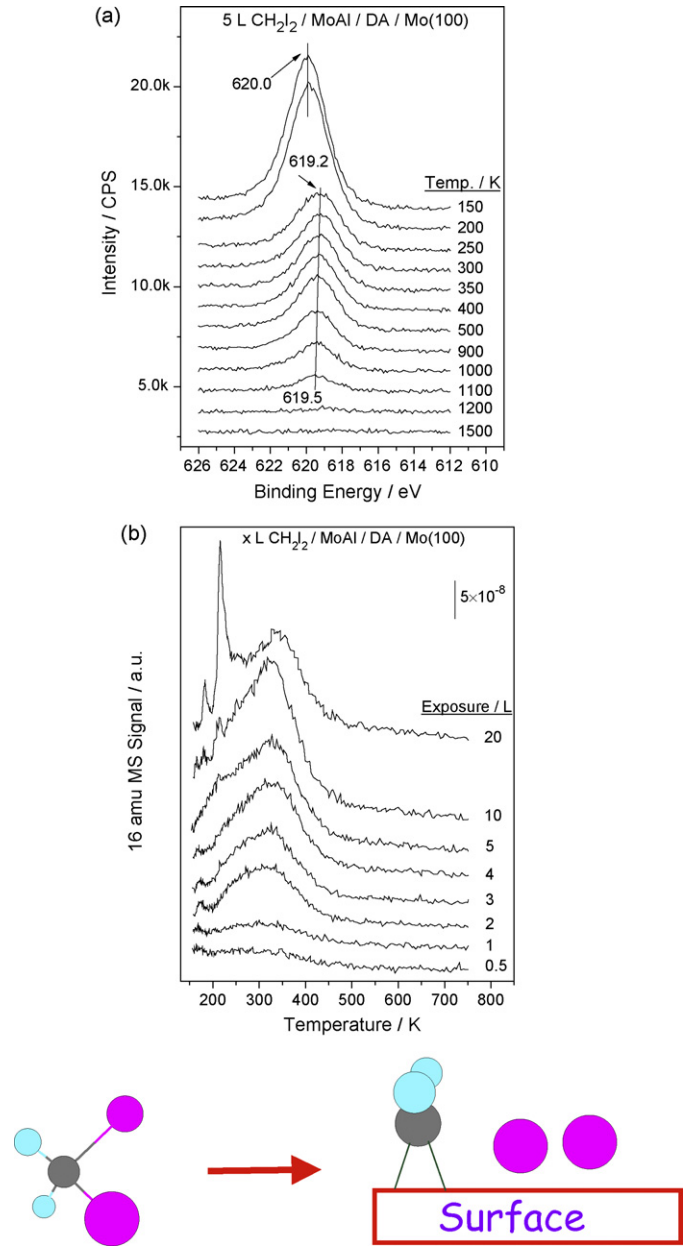

Fig. 8. (a) *I3d* regions collected following the adsorption of 5 L of diiodomethane on a MoAl alloy film at 150 K and heating to various temperatures, where annealing temperatures are marked adjacent to the corresponding spectrum. The spectra were collected after allowing the sample to cool to 150 K. (b) 16 (CH_4) amu temperature-programmed desorption spectra of diiodomethane adsorbed on a MoAl film at 150 K collected using a heating rate of 10 K/s, as a function of CH_2I_2 exposure. Diiodomethane exposures are marked adjacent to the corresponding spectrum. The surface chemistry is indicated schematically at the bottom of the figure.

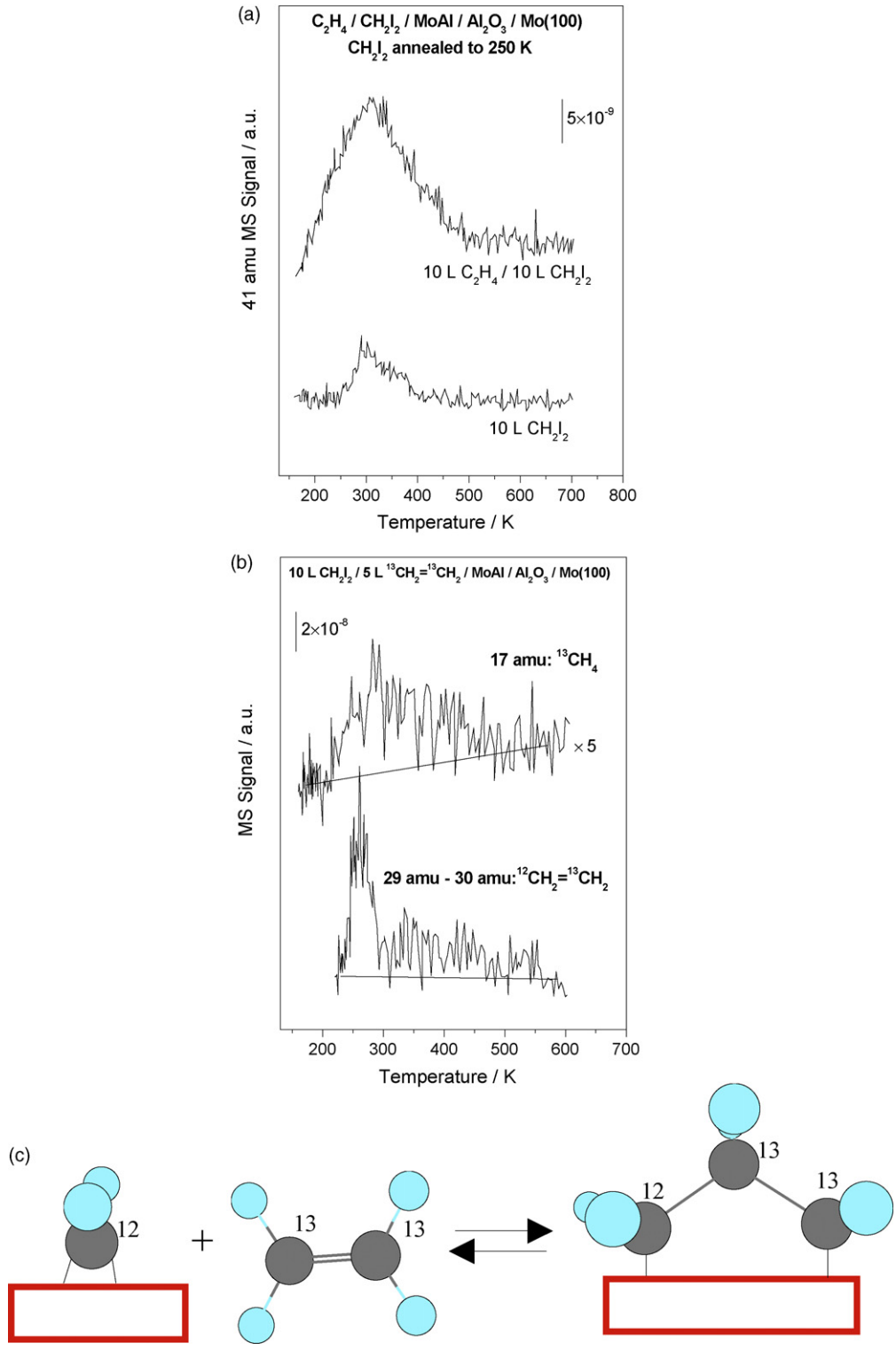

Fig. 9. Temperature-programmed desorption spectra collected using a heating rate of 10 K/s, (a) monitoring 41 amu (propylene) following adsorption of 10 L of methylene iodide and annealing to 250 K to form a methylene species, followed by exposure to 10 L of ethylene to this surface. Shown for comparison is the spectrum of methylene iodide alone. (b) The spectra obtained following adsorption of 5 L of $^{13}C_2H_4$ followed by 10 L of $^{12}CH_2I_2$, monitoring 17 ($^{12}CH_4$) and 29 amu ($^{12}C^{13}CH_4$) where contributions from molecular ethylene have been subtracted, and (c) the 41 amu (propylene) spectrum following exposure to 1 L of C_2H_5I followed by 1 L CH_2I_2. The surface chemistry is indicated schematically at the bottom of the figure.

signal at 41 amu with fragments at 27 and 26 amu. However, comparison of the relative intensities at 26 and 27 amu for the metallacycle with the intensity at 41 amu reveals that the 26 and 27 amu intensities are larger than can be accounted for by propylene alone, suggesting that the metallacycle also decomposes to yield ethylene. This notion is confirmed by the TPD spectra collected following 5 L exposure of 1,3-diidodopropane, which shows clearly different desorption profiles at 26 and 27 amu to

that at 41 amu, indicating that ethylene is formed at ∼280 K. Monitoring the 16 amu signal (Fig. 7(b)) reveals the formation of substantial amounts of methane between 250 and 300 K. As will be shown below, this is due to the hydrogenation of methylene species deposited onto the surface by the decomposition of the metallacycle. The reaction chemistry is summarized schematically at the bottom of Fig. 7.

Methylene species can themselves be grafted onto the alloy surface using a similar strategy, by exposing it to methylene iodide [12]. The XP spectra displayed in Fig. 8(a) confirm that adsorbed methylene iodide, with an iodine signal at ∼620.0 eV binding energy, decomposes on heating to ∼200 K as evidenced by the appearance of an iodine signal at ∼619.5 eV, due to iodine adsorbed onto the alloy. The resulting 16 amu (methane) TPD data are displayed in Fig. 8(b), showing methane desorption at ∼300 K, in accord with the proposal that the methane detected following 1,3-diidodopropane adsorption is due to $CH_{2(ads)}$ hydrogenation (Fig. 7(b)).

In order to explore whether methylene species insert into the C–metal bond of adsorbed ethylene to form a metallacycle, carbenes were formed on the surface by adsorbing methylene iodide at ∼100 K and annealing to 250 K [43]. The surface was then exposed to ethylene and the resulting 41 amu (propylene) TPD data are displayed in Fig. 9(a). This displays an intense feature centered at ∼320 K consistent with the decomposition of a C_3 metallacycle (compare with Fig. 7(a)). As noted above, higher hydrocarbons are formed from adsorbed methylene species due to migratory insertion reactions into alkyl species and the 41-amu spectrum for methylene iodide alone on the alloy surface is shown also in Fig. 9(a). In this case, the propylene yield is substantially lower than when co-adsorbed with ethylene. These results strongly suggest the formation of metallacycles by reaction between carbenes and adsorbed ethylene in agreement with the proposed pathway for olefin metathesis in heterogeneous phase [13–30]. The data of Fig. 7(a) indicate that these can also decompose to reform the surface carbene and evolve and alkene. In order to establish whether this cross metathesis pathway indeed occurs on the alloy surface, the carbene was graft onto the surface using $^{12}CH_2I_2$ and co-adsorbed with isotopically labeled $^{13}C_2H_4$. As indicated in the schematic at the bottom of Fig. 9, the resulting metallacycle should contain two ^{13}C and one ^{12}C atoms. In this case, there is a 50% probability of the metallacycle decomposing to yield the original reactants and a 50% probability of yielding $^{12}C^{13}CH_4$ and depositing $^{13}CH_2$ species onto the surface. The results of this experiment are displayed in Fig. 9(b), where a clear signal due to cross-metathesis products is detected. In addition, according to the results shown in Fig. 8, the resulting ^{13}C-labeled methylene species should hydrogenate to produce labeled methane (at 17 amu) and this is indeed found (Fig. 9(b)). The results indicate that the carbene–metallacycle pathway proposed by Hérisson and Chauvin [17] for homogeneous-phase olefin metathesis can also occur in heterogeneous phase.

4. Conclusions

The experimental results provide clear evidence for ethylene insertion into the acetate proceeding *via* a pathway proposed by Samanos [32], that is, by ethylene insertion into an adsorbed acetate species and subsequent β-hydride elimination to form vinyl acetate. First is the identification of a vibrational mode at $\sim 1718\,cm^{-1}$ when reaction is carried out using C_2D_4, which cannot be assigned to vinyl acetate itself and is therefore assigned to the acetoxyethyl-palladium intermediate. Second, the differences in reaction rates for CHDCHD and CH_2CD_2 can only be rationalized by the Samanos route by making the reasonable assumption that the acetoxyethyl-palladium intermediate blocks the adsorption of ethylene. Molybdenum–aluminum alloys grown by reacting $Mo(CO)_6$ with thin alumina films on a refractory metal support have been shown to be very active for methylene insertions reactions. This observation was exploited to explore the Hérisson-Chauvin [17] reaction pathway for olefin metathesis that proposes a reaction between an alkene and carbene to form a metallacycle that decomposes by the reverse of this pathway to form metathesis products. This reaction pathway was confirmed on the alloy surface by grafting key intermediates onto the surface using iodine-containing precursors.

Acknowledgements

We gratefully acknowledge support of this work by the U.S. Department of Energy, Division of Chemical Sciences, Office of Basic Energy Sciences, under Grant No. DE-FG02-92ER14289 and by the Chemistry Division of the National Science Foundation under grant number CTS-0105329.

References

[1] U.S. Patent 365,888 (1967).
[2] Y.F. Han, D. Kumar, C. Sivadinayarana, D.W. Goodman, J. Catal. 224 (2004) 60.
[3] M. Kaltchev, W.T. Tysoe, J. Catal. 193 (2000) 29.
[4] M. Kaltchev, W.T. Tysoe, Top. Catal. 13 (2000) 121.
[5] M. Kaltchev, W.T. Tysoe, J. Catal. 196 (2000) 40.
[6] Y. Wang, F. Gao, M. Kaltchev, D. Stacchiola, W.T. Tysoe, Catal. Lett. 91 (2003) 83.
[7] Y. Wang, F. Gao, M. Kaltchev, W.T. Tysoe, J. Mol. Catal. A: Chem. 209 (2004) 135.
[8] Y. Wang, F. Gao, W.T. Tysoe, J. Mol. Catal. A: Chem. 236 (2005) 18.
[9] Y. Wang, F. Gao, W.T. Tysoe, J. Mol. Catal. A: Chem. 235 (2005) 173.
[10] F. Gao, Y. Wang, W.T. Tysoe, J. Mol. Catal. A: Chem. 236 (2005) 18.
[11] Y. Wang, F. Gao, W.T. Tysoe, J. Mol. Catal. A: Chem. 248 (2006) 32.
[12] Y. Wang, F. Gao, W.T. Tysoe, J. Phys. Chem. B 109 (2005) 15497.
[13] G.S. Lewandos, R. Pettit, J. Am. Chem. Soc. 93 (1971) 7087.
[14] R.H. Grubbs, T.K. Brunck, J. Am. Chem. Soc. 94 (1972) 2538.
[15] B.M. Novak, R.H. Grubbs, J. Am. Chem. Soc. 110 (1988) 960.
[16] C.G. Biefeld, H.A. Eick, R.H. Grubbs, Inorg. Chem. 1973 (1973) 12.
[17] J.-L. Hérisson, Y. Chauvin, Makromol. Chem. 141 (1971) 161.
[18] J.-P. Soufflet, D. Commereuc, Y. Chauvin, C.R. Hebd, Seances Acad. Sci. Sér. C 276 (1973) 169.
[19] D.J. Cardin, M.J. Doyle, L.F. Lappert, J. Chem. Soc., Chem. Commun. (1972) 927.
[20] C.P. Casey, T.J. Burkhardt, J. Am. Chem. Soc. 96 (1974) 7808.
[21] T.J. Katz, J. McGinnis, J. Am. Chem. Soc. 97 (1975) 1592.
[22] R.H. Grubbs, P.L. Burk, D.D. Carr, J. Am. Chem. Soc. 97 (1975) 3265.
[23] J. McGinnis, T.J. Katz, S. Hurwitz, J. Am. Chem. Soc. 98 (1976) 605.
[24] T.J. Katz, J. McGinnis, C.J. Altus, J. Am. Chem. Soc. 98 (1976) 606.
[25] J.H. Wengrovius, J. Sancho, R.R. Schrock, J. Am. Chem. Soc. 103 (1981) 3932.
[26] T. Masuda, H. Sasaki, T. Higashimura, Macromolecules 8 (1975) 717.

[27] T.J. Katz, S.J. Lee, J. Am. Chem. Soc. 102 (1980) 422.
[28] T.J. Katz, T.M. Sivavec, J. Am. Chem. Soc. 107 (1985) 737.
[29] R.R. Schrock, J. Organometal. Chem. 300 (1986) 249.
[30] S.T. Nguyen, L.K. Johnson, R.H. Grubbs, J.W. Ziller, J. Am. Chem. Soc. 114 (1992) 3974.
[31] F. Calaza, F. Gao, Z. Li, W.T. Tysoe, Surf. Sci. 601 (2007) 714.
[32] B. Samanos, P. Boutry, R. Montarnal, J. Catal. 23 (1971) 19.
[33] I.I. Moiseev, M.N. Vargaftic, Y.L. Syrkin, Dokl. Akad. Nauk. USSR 133 (1960) 377.
[34] James, D.K. Saldin, T. Zheng, W.T. Tysoe, D.S. Sholl, Catal. Today 105 (2005) 74.
[35] T. Zheng, D. Stacchiola, H.C. Poon, D.K. Saldin, W.T. Tysoe, Surf. Sci. 564 (2004) 71.
[36] D. Stacchiola, L. Burkholder, W.T. Tysoe, Surf. Sci. 511 (2002) 215.
[37] M. Kaltchev, A.W. Thompson, W.T. Tysoe, Surf. Sci. 391 (1997) 145.
[38] R.D. Haley, M.S. Tikov, R.M. Lambert, Catal. Lett. 76 (2001) 125.
[39] D. Stacchiola, F. Calaza, L. Burkholder, W.T. Tysoe, J. Am. Chem. Soc. 126 (2004) 15384.
[40] F. Calaza, D. Stacchiola, M. Neurock, W.T. Tysoe, Surf. Sci. 598 (2005) 263.
[41] L.J. Bellamy, The Infrared Spectra of Complex Molecules, John Wiley and Sons, New York, 1959.
[42] T. Bürgi, J. Catal. 229 (2005) 55.
[43] F. Gao, Y. Wang, W.T. Tysoe, J. Am. Chem. Soc. 128 (2006) 7091.